Biomedical Signal Processing and Control 48 (2019) 69–79

Contents lists available at ScienceDirect

Biomedical Signal Processing and Control

journal homepage: www.elsevier.com/locate/bspc

Color perception algorithm of medical images using density peak based hierarchical clustering

Xianhua Zeng*, Aozhu Chen, Meng Zhou

Chongqing Key Laboratory of Computational Intelligence, College of Computer Science and Technology, Chongqing University of Posts and Telecommunications, Chongqing 400065, China

ARTICLE INFO

Article history:
Received 17 April 2018
Received in revised form 25 August 2018
Accepted 27 September 2018
Available online 15 October 2018

Keywords:
Multi-feature fusion
Density peak
Medical image
Color perception

ABSTRACT

In this paper, we present a method which can generate color medical images based on multi-feature fusion and hierarchical density peak clustering. First, the proposed method extracts multi-feature to gain abundant feature information. Then, select the regional representative pixels utilizing the local density and neighborhood relationship of pixels. Next, color information is embedded to regional representative pixels. Finally, obtain the color information of each pixel according to the similarity of the representative pixel and non-representative pixel. The experiments on CT, MRI, PET, Ultrasound and DTI demonstrate that the color medical images generated by the proposed algorithm have exquisite details and clear texture information. Moreover, the complexity of the proposed method is $O(MN)$, lower than $O(N^3)$ (DPDR). Compared with other corresponding methods, the proposed method has higher contrast, average gradient and lower information entropy.

1. Introduction

The development of medical imaging technology has been promoted by medical equipment and computer hardware, and a large number of high quality medical images are produced. Various multimodal medical images like CT (computed tomography), MRI (magnetic resonance imaging), PET (positron emission tomography), DTI (diffusion tensor images) etc., are widely used in clinical procedures, and most of which are grayscale images [1]. These medical images only use light and shade to express the physiological information, however, human eyes can hardly distinguish the slight changes in the grayscale, which result in losing or hiding useful details of medical images and bringing diagnostic difficulties [2]. Therefore, it is very necessary to enhance the monochromatic medical modality into colorized images. Increasing the details and emerging the features are helpful to improve the visual effect of medical images and make them more discriminative.

Colorization of medical images technology is a hot research worldwide in medical images processing. In [3], Welsh et al. introduced a general technique for colorizing grey-scale images by transferring color between a color reference image and a grayscale image. However, the method coloring images only depends on luminance channel and the standard deviation of neighborhood region of pixels. In [4], Brun et al. proposed a method for coloring DTI fiber traces using Laplacian Eigenmaps (LE) to enhance the perception fiber bundles and connectivity in human brain. This study focuses only on fiber traces rather than grayscale medical images. In [5], X.H. Xiao et al. presented an approach which transferred color information using a rotation matrix, so that this approach can borrow one images color characteristic from another in any three dimension color space directly. In [6], Pitie et al. proposed an iterative method for grading the colors between different images by transforming any N-dimensional probability density function into another one, and running a post-processing algorithm to reduce the grain artefacts of the outcomes. In [7], Hamarneh et al. applied the Isometric Mapping for visualizing manifold-valued DTI images in the form of color images (DPDR). A novel visualization approach of DTI follow in DPDR has proposed in [8]. The merit of that method is local preserving dimensionality reduction, and then mapping the low dimension data to RGB space to gain color images. In [9], a color transfer framework to evoke different emotions for images based on color combinations are proposed. Whereas they only use three color combinations, which are not adaptive to the number of colors of reference image. Literature [10] proposed an approach for color perception of DTI based on hierarchical manifold learn-

* Corresponding author.
E-mail addresses: zengxh@cqupt.edu.cn (X. Zeng), 476170194@qq.com (A. Chen), 314444586@qq.com (M. Zhou).

https://doi.org/10.1016/j.bspc.2018.09.013
1746-8094/

ing(CPDTIHML), which can reduce the computation complexity from $O(N^3)$ [7] to $O(N^2)$.

However, the luminance feature of grayscale medical images only has 256 gray shades variations, showing a poor visualization [11]. In this paper, we extract a multi-directional gradient feature from grayscale medical images and fuse it with luminance feature of the original medical image to obtain a high dimensional data. Based on the CPDTI-HML, taking advantage of the gradient feature of different directions in medical images and combining clustering by fast search and find of density peaks(DPClust) [12], we propose a color perception algorithm of medical images named CPMI-DPHC. First, select the pixels that represent the local region by local density, the local density is defined in DPClust. Then use color perception of representative pixels to obtain the color information of all pixels. The main contributions of this paper are: (a) the proposed method enriches medical image information by extracting multi-directional gradient features, which addresses the problem of poor feature information; (b) the proposed method reduces the computation complexity from $O(N^2)$ to $O(MN)$, where $M \ll N$, therefore $O(MN)$ is larger than $O(N)$ but smaller than $O(N^2)$; (c) the proposed method not only work on diffusion tensor images, but also can work on normal grayscale medical images.

The method is summarized in the following steps: Step 1, extract the gradient features of grayscale medical images; Step 2, cluster all the pixels with the various features to gain the regional representative pixels; Step 3, map the regional representative pixels to a three dimensional space with the manifold learning method; Step 4, rotate the coordinates from the three-dimensional space to RGB color space; Step 5, spread color information to all pixels. The detailed description of the proposed method is shown in Section 3. The dataset, experimental settings, experimental results, and the analysis of the results are detailed in Section 4. The discussion about the proposed method is described in Section 5. Finally, we describe the conclusion and the future work in Section 6.

2. Related works

To the best of our knowledge, the works mostly related to our approach are those of DPDR [7] and CPDTI-HML [10]. The method of DPDR involves distance-preserving dimension reduction and color perception for DTI, which renders the different perceptual colors to accurately reflect the different high-dimensional pixel values [13]. First, the method computes the geodesic distance of any two pixels on the high dimensional manifolds to obtain the similarity of the two pixels. Then, the distance preserving is applied to map the high-dimensional space to the three-dimensional space. Finally, the lower dimensional coordinates in the three-dimensional space are mapped to the three-channel color space. However, DPDR only focuses on color differences among pixels but ignores the structure of object, which causes high computational cost because of the calculation of the geodesic distance of pixels. Considering that the distance-preserving dimensionality reduction for coloring perception DTI is rational but the computational cost is high, CPDTI-HML involves color perception of diffusion tensor images using hierarchical structure, which is derived from the Algebraic Multigrid. The method of CPDTI-HML constructs a hierarchical structure for all the pixels of the underlying pixel by filtering the representative points. From the bottom to top, the method forms a pyramid, in which the most valuable pixels are at the top, and then using the Multidimensional scaling (MDS) [14] map the top-layer representative pixels to a lower dimension space and convert those lower dimension coordinates to the RGB color space. In addition, make sure that the colors of similar areas as close as possible, and dissimilar regions have different colors. Finally, interpolate the top-layer pixels to all nodes in the bottom layer. However, CPDTI-HML repeatedly calculates similarity matrix and only considerate the threshold when building a hierarchical structure. Furthermore, both of them are only apply to DTI.

3. Method

DPDR has high computational cost and lacks of regional structures, to address those issues, we propose a method mainly based on CPDTI-HML and use clustering method to find the representative pixels from the bottom directly. Different from the DTI, the ordinary grayscale medical images have no high-dimensional features. So we extract the gradient features of grayscale medical images to obtain the high dimensional data that contains more exquisite information of grayscale medical images. Besides, clustering with the various features of each pixel can separate the regional structure of the images. The proposed method further improves the computational efficiency of DPDR algorithm, and achieves more comprehensive and better images by the regional representative pixels. First, cluster the informative multi-feature medical image data, and select the regional representative pixels. The regional representation pixels are mapped to a three-dimensional space using the manifold learning method. Then, convert those pixels to the RGB color space. Last, the color information of all pixels is obtained according to the similarity between pixels. Fig. 1 presents the overview of the proposed algorithm.

3.1. Feature extraction of medical images

Medical image fusion technology can achieve more interpretable images by integrating the complementary information of medical images, which can provide more accurate information for

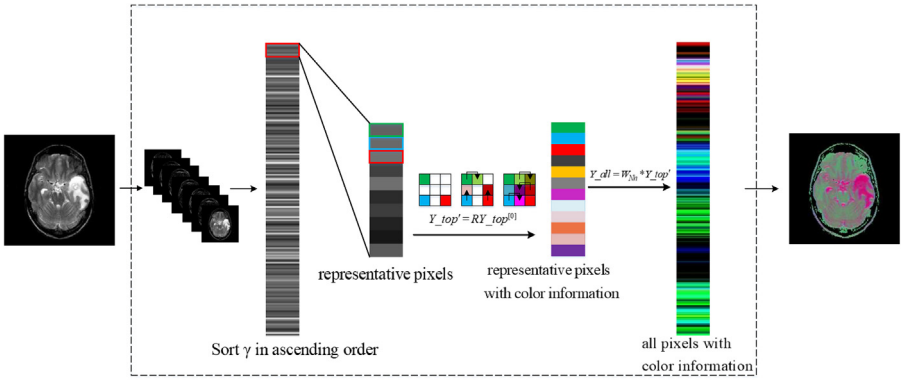

Fig. 1. The overview of the proposed algorithm.

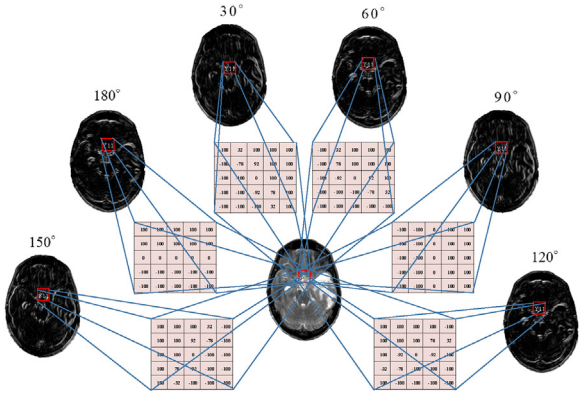

Fig. 2. Multi-directional features extraction of grayscale medical image.

clinical diagnosis and treatment [15]. In order to maintain the original medical image structure to display more edges and details in medical images, we can restore the physiological information contained in medical images more truly. In this paper, we extract multi-directional gradient features of the gray medical images and fuse with its luminance feature. Since the image is stored in a matrix and all the gradient of the image is used to represent the edge of the image [16]. The magnitude of the convolved output and the direction of the mask giving the highest output at each pixel are recorded as edge data, we use the mask to convolution the original image to achieve the desired effect. In general, the smaller masks are sensitive to noise, whereas the larger masks cannot resolve fine detail and the computational cost may be prohibitive [17]. Because the mask of 3×3 involved in the filtering operation is very small, and the gradient operator of the small window is only associated with the small area in the image, the gradient feature of the calculation only contains a very small amount of context regional information related to the original image. Therefore, the gradient features which calculated by 3×3 are coarse. The mask of 7*7 can gain more detailed direction gradient information and the larger context area information, but the computation of the mask of the 7×7 is much larger than that of the 3×3 and the 5×5. Compared with the 3×3 operator, the 5×5 operator obtains more information about the directional gradient information and the context area information when the computation increases slightly. Compared with the 7×7 operator, 5×5 has less computation, although the information contained in the 5×5 operator is smaller. Finally, considering the amount of computation, the gradient information contained in the feature and the context information, we choose the 5×5 operator as a compromise. In this paper, we use a 5×5 operator proposed by Nevatia et al. [18], which adjust the direction by using the weight of each position. In the literature [18], the author verifies the feasibility and superiority of the mask. The 12 filters of the Nevitia operator represents 12 directions and gives the maximum response to 12 specific edge directions on the image, and then it take the maximum value as the edge output of the image. Since the first six filters and the last six filters of Nevitia operator are symmetric, we only use the first six filters to gain the gradient features of the original grayscale medical image. The gradient feature extraction process of grayscale medical image is shown in Fig. 2.

3.2. Selection of regional representative pixels

In the DPDR method, there is a high computational complexity. Therefore, the CPDTI-HML method selects representative seeds to reduce computation complexity, but ignores the region information of the image during constructing the hierarchical layer. To inherit the merits of lower computation from CPDTI-HML, we use clustering algorithm to find the representative pixels to avoid repeat calculation of similarity matrix and to guarantee the stability of regional structure. In this paper, a representative pixel is chosen based on the principle of clustering by fast search and find of density peaks (DPClust) [12]. Clustering every pixel with its neighbor pixels into a same cluster, and then find the density peaks of every cluster and use them as the regional representative pixels. Our approach select regional representative pixels based on DPClust, so we introduce those papers idea and algorithm here briefly.

DPClust based on the idea that cluster centers are characterized by a higher density than their neighbors and by a relatively large distance from points with higher densities [19]. It means that regional representative pixels (cluster centers) are always surrounded by non-representative pixels, and that the distance between two regional representative pixels is relatively far. Selecting regional representative pixels in this way, the larger distance between the representative pixels can maximize the differences between different blocks, in consequence of the smaller the similarity and the greater color difference after color perception.

Calculating the distance matrix $d_{i,j}$ between all pixels via

$$d_{i,j} = \|x_i - x_j\|^2, \quad 1 \le i < j \le N, \quad x \in R^\tau, \tag{1}$$

where x_i denotes the pixels, τ is the dimensions of pixels and N is the number of pixels.

The authors of DPClust stated that the results of cluster are robust with respect to the choice of d_c when a Gaussian kernel is used. So we use Gaussian kernel rather than cut-off kernel. Computing the local density ρ_i of each pixels, via

$$\rho_i = \sum_{j \in I \setminus \{i\}} e^{-\left(\frac{d_{i,j}}{dc}\right)^2}, \quad I = 1, \ldots, N. \tag{2}$$

Where d_c is the cutoff distance. After getting the density ρ_i, sort $\rho_i = \{\rho_1, \rho_2, \ldots, \rho_N\}$ in descending order to obtain $\boldsymbol{\rho} = \{\rho_{q_1}, \rho_{q_2}, \ldots, \rho_{q_N}\}$, and the $\{q_1, q_2, \ldots, q_n\}$ is the sorted indexes of ρ in descending order.

The distance between a pixel and its nearest points with higher local density is defined as follows:

$$\delta_{q_i} = \begin{cases} \min\limits_{j<i} \left\{ d_{q_i,q_j} \right\}, i \ge 2; \\ \max\limits_{j \ge 2} \left\{ d_{q_i,q_j} \right\}, i = 1. \end{cases} \tag{3}$$

We define each pixel's nearest neighbor of higher density as *DNn*. After getting the distance δ_{q_i}, set index of the *DNn* with the maximum density to 0, write the index of the *DNn* in the vector *DNn* as:

$$DNn_i = \begin{cases} \{0 | i = q_1\} \\ \{j | \delta_i = d_{i,j}, i \in \{q_2, \ldots, q_N\}\} \end{cases}. \tag{4}$$

In order to facilitate the selection of cluster centers, an instrumental variable γ_i [19] is calculated to ensure that the distance between two regional representative pixels is relatively long. The variable is defined as:

$$\gamma_i = \rho_i \cdot \delta_i. \tag{5}$$

First, put each pixel in an individual cluster, and start from the pixel where the value of γ_i is minimum and merge it with its nearest neighbor with higher density DNn_i, and then merge pixels with their *DNn* in the sequence of an ascending order of γ_i. If the pixel has been merged in this round of merge, just skip to next pixel. After first round merge, select the pixels which have maximum γ_i as the center of each cluster. Pixels or clusters of pixels are then successively merged until the representative pixels(cluster centers) no longer changes. At each iteration, according to the *DNn* of the clus-

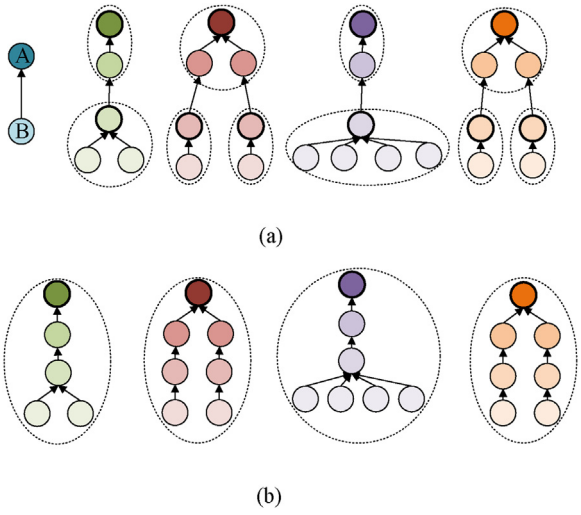

Fig. 3. The process of merging.

ter center, merge the two clusters in which the cluster center and its *DNn* is located into one cluster.

The clustering process of pixels is shown in Fig. 3, where the thicker dots are cluster centers. Dot A point to dot B to indicate that the pixel B is the nearest neighbor of pixel A, the pixels in the same dotted line are represented in the same cluster. Clusters merge with the cluster which contain the nearest neighbor of their cluster center. This can be illustrated by Fig. 3a and b. Fig. 3a is the *k*th clustering results, Fig. 3b is the $k+1$th clustering results.

3.3. Color perception of pixel

The color space is three-dimensional space, for the regional representative pixels, we use Multidimensional scaling (MDS) [14] to gain the three-dimension coordinates. MDS is a globality preserving method, which uses the similarity between paired samples to construct suitable low dimensional space, so that the similarity between samples in this space and those in high dimensional space can be kept as consistent as possible.

The color medical image structure after coloring should be as close as possible to the structure of the original medical image, while processing the high dimensional data, we introduce the concept of feature weight ω [20], making different features have different importance to preserve crucial information in the original medical image. Thus, the distance for regional representative pixel is defined as follows:

$$D_{R_{i,j}} = \sqrt{\sum_{k=1}^{\tau} \omega^k (c_i^k - c_j^k)^2}\ , \tag{6}$$

where $D_{R_{i,j}}$ denotes the distance of regional representative pixel,τ denotes the dimension of pixels, c_k^i denotes the *k*th feature of the *i*th representative pixel.

After obtaining the distance $D_{R_{i,j}}$, the MDS used for distance-preserving mapping to gain the three dimension coordinates as

$$Y = \left(\sqrt{\lambda_1}v_1^T, \sqrt{\lambda_2}v_2^T, \sqrt{\lambda_3}v_3^T\right)^T, \tag{7}$$

where λ_1, λ_2, λ_3 denote maximum eigenvalues of the distance matrix $D_{R_{i,j}}$, and v_1, v_2, v_3 denote the eigenvectors corresponding to the eigenvalues.

The three dimensional coordinates of representative are converted to the RGB color space via the rotation-scaling transformation matrix *R* [21], which must be satisfied with the formula:

$$R = USV^T. \tag{8}$$

In order to calculate the rotation-scaling transformation matrix *R*, we initialize different color information C_s to three representative pixels. Then get the covariance matrix σ of the three-dimensional coordinates Y_S of the corresponding representative pixels via

$$\sigma = \frac{1}{3}\sum_{i=1}^{3}\left(C_s - \mu_{C_s}\right)\left(Y_s - \mu_{Y_s}\right)^{\mathrm{T}}, \tag{9}$$

where the μ_{C_s} denotes means of initialize color information C_s and the μ_{Y_s} denotes means of three dimensional coordinates Y_s. The singular value decomposition of the covariance matrix σ is USV^T, and the *S* is defined as

$$S = \begin{cases} UU^T \ \ or \ \ VV^T, & |\sigma| \geq 0 \\ \mathrm{diag}(1, 1, -1), & otherwise \end{cases}. \tag{10}$$

Which means if the determinant$|\sigma| \geq 0$ is a 3×3 unit matrix, it means that the same direction rotation is used, otherwise the different direction rotation is used.

Through the above calculation, the rotation scaling transformation matrix *R* is obtained. Then gain the color information of all representative pixels via

$$Y\_top' = RY\_top[0], \tag{11}$$

where the $Y\_top[0]$ denotes the 3-dimension coordinates of representative pixels, and Y_top' denotes the color information of representative pixels.

The similarity matrix W_R between representative pixels and non-representative pixels defined as follows:

$$W_R = \begin{cases} \exp\left(-\sqrt{\sum_{k=1}^{\tau}\omega^k (I_i^k - c_j^k)^2}\right), & i \in nearestneighbor(j) \\ 0, & i \notin nearestneighbor(j) \end{cases}, \tag{12}$$

where I_i^k denotes all pixels, $nearestneighbor(j)$ denotes the nearest neighbor pixel of the *j*th representative pixel.

The color information of the representative pixels is spread to all pixels via

$$Y\_all = W_R Y\_top', \tag{13}$$

where Y_all denotes the color information of all the pixels.

In this manner, use the similarity matrix weight the color information of the representative pixel to get the color information of all the pixels in the bottom, so that, a complete color medical image is formed.

3.4. Summary of the proposed algorithm

The work presented in this paper focuses on increasing computational efficiency of DPDR and generating color medical images with exquisite details and clear texture. We present a framework to process various grayscale medical images. First, extract the gradient features of the grayscale medical image in six directions and fuse it with luminance feature. Then find the representative pixels adopt the density peak based hierarchical clustering. Next, map the coordinates of representative pixels to the RGB color space. Finally, return the color information to all pixels via the similarity matrix between representative pixels and non-representative pixels. It is noteworthy that, the part of dimensionality reduction

of representative pixels can be employed to various manifold learning method. The distance preserving projection is generally the preferred method by virtue of the fact that the representative pixels are distant which not applicable for neighborhood preserving. The main procedures of the proposed method are summarized in Algorithm 1.

Algorithm 1. Color perception algorithm of medical images using hierarchical clustering based density peak

Input: Grayscale medical image
Output: Color medical image
1: Generate gradient features in six direction
2: Compute distance matrix $d_{i,j}$ between all pixels using the gradient features and luminance features
3: Use $d_{i,j}$ and cutoff distance d_c to compute the local density ρ_i by Eq. (2)
4: Gain the distance between a pixel and its nearest points with higher local density δ_{q_i} and the nearest neighbor with larger local density Nn_i by Eqs. (3) and (4) respectively
5: Compute instrumental variable γ_i via elementwise product of ρ_i and δ_i
6: Place each input pixels in an individual cluster
7: **repeat**
8: Select the cluster center which has the largest in their cluster to represent their cluster
9: Merge the two cluster in which the cluster center and its nearest neighbor is located into one cluster
10: Output the cluster center of each cluster to be the representative pixels
11: **until** Number of representative pixels is no longer changed
12: Obtain the similarity matrix W_R via Eq. (12)
13: Compute the three-dimensional coordinates of representative pixels
14: Transform color information using rotation-scaling transformation matrix R
15: Color information of all pixels gained by Eq. (13)

3.5. Complexity analysis of the proposed algorithm

The major cost of our method is mainly concerned with the three groups: the complexity of feature extraction $T(N)_1$, the complexity of selection of representative pixels $T(N)_2$ and the complexity of color perception of pixels $T(N)_3$.

In this paper, we convolve on the grayscale medical image with 6 different orientation convolution kernels of size 5*5 to perform multi-feature extraction. We use weighted summation 25 times by one convolution, the convolution kernel slide $(m-5+1)*(n-5+1)$ times on the image. Therefore, the complexity of feature extraction is $T(N)=T(6*25*(m-5+1)(n-5+1))=O(mn)$. Where m, n respectively represents the height and width of image. Set $m \times n$ as N which is the number of pixels, the complexity simple to $T(N)_1=O(N)$.

In the process of representing pixels selection, N denotes the total number of all pixels. In the best case, the representative pixels can be obtained by first iteration, we just need traverse N pixels once, so that the complexity is $O(N)$. In the worst case, we merge two clusters into one at each iteration, we should traverse every pixels of N pixels, so the complexity of first iteration is $O(N)$. In this case, we cluster N pixels into $N/2$ clusters after first iteration, and cluster $N/2$ clusters into $N/4$ in the second iteration, and so on, until to the end of clustering. Stated thus, the complexity can be expressed by the following equation:

$$T(N)=T\left(\frac{N}{2}\right)+O(N)=T\left(\frac{N}{4}\right)+O\left(\frac{N}{4}\right)+\cdots+O(N)+\cdots \quad (14)$$

According the formula of summation for geometric sequence, and the Master Method in [22]. The K denotes the Kth iteration.

$$\begin{aligned}
T(N) &= T\left(\frac{N}{2}\right)+O(N)\\
&= T\left(\frac{N}{2^K}\right)+O\left(\frac{N}{2^K}\right)+\cdots+O\left(\frac{N}{2}\right)+O(N)\\
&= \lim_{K->+\infty}\left(T\left(\frac{N}{2^K}\right)+O\left(\frac{N}{2^K}\right)+\cdots+O\left(\frac{N}{2}\right)+O(N)\right)\\
&= \lim_{K->+\infty}T\left(\frac{N}{2^K}\right)+\lim_{K->+\infty}\sum_{i=0}^{K}O\left(\frac{N}{2^i}\right)\\
&= T(0)+\lim_{K->+\infty}\sum_{i=0}^{K}O\left(\frac{N}{2^i}\right)\\
&= \lim_{K->+\infty}\sum_{i=0}^{K}O\left(\frac{N}{2^i}\right)\\
&= \lim_{K->+\infty}O\left(\frac{(1-\frac{1}{2^K})N}{1-\frac{1}{2}}\right)\\
&= O(2N)=O(N)
\end{aligned}$$

For the color perception of pixels, the complexity is reflected in the transfer of color information between the representative pixels and non-representative pixels. Suppose that N denotes the number of all pixels, M denotes the number of representative pixels. As the Eq. (13) implies, matrix multiplication between two matrix. The size of them is $N*M$ and $m*3$. According to the complexity of matrix multiplication, the complexity of this process is $T(N)_3=O(MN)$.

According to the above analysis, the complexity of the proposed method $T(N)$ can be calculated as follows:

$$\begin{aligned}
T(N) &= T(N)_1+T(N)_2+T(N)_3\\
&= O(N)+O(N)+O(MN)\\
&= O(MN)
\end{aligned} \quad (15)$$

where the N denotes the number of pixels, and the M denotes the number of representatives pixels, and $M \ll N$.

Normally, the complexity of CPMI-DPHC is $O(MN)$, it decreases the complexity of calculation compared with methods in the literature [7] from $O(N^3)$ to $O(MN)$ and the $O(MN)$ is less than $O(N^2)$ [10].

4. Experiments

In order to verify the effectiveness and superiority of the proposed method, we have carried out a grouping experiment on multiple modality medical images with the Matlab. In this section, we apply the MDS and Laplacian Eigenmaps (LE) [23] to obtain the different three dimensional coordinates of representative pixels respectively. The experiment is intended to show that the algorithm of dimensional reduction in our method is not just confined to MDS. LE constructs the relationship between the local neighborhoods of data, so that the data of the nearest neighbor in the high dimensional space is as close as possible after the dimensionality reduction. After being embedded into a low dimensional subspace, the samples of the same class maintain their intrinsic neighbor relations, while the samples of the different classes are far from each other. At this point, it's remarkable that the color of outcomes can be influenced by the eigenvector and eigenvalue of the Laplace matrix. Because the Laplace matrix is huge, but the eigenvalues are small, even close to zero, so the minimum value of the eigenvalue decomposition is varied. In consequence of the unstable minimum value

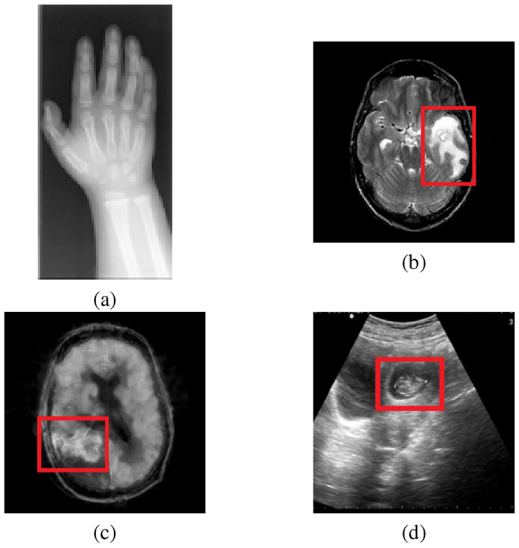

Fig. 4. Original medical images. (a) CT, (b) MRI, (c) PET, (d) Ultrasound.

of the eigenvalue decomposition, the color of the result generated by our method in each run will be different.

4.1. Dataset

The approach is tested on several medical images such as CT, MRI and PET acquired from open source on Harvard Medical School [24], and the Ultrasound images coming from a 3-A major Hospital in Chongqing, China, collected from 2014 to 2015. CT images are represented by different grayscales, reflecting the absorption of X rays by organs and tissues. MRI images are very similar to those of CT images. The two are "digital images" and show dissected and pathological section images of different structures with different gray levels. PET is the most advanced clinical examination and imaging technology in nuclear medicine. PET is the only technique to perform functional, metabolic and receptor imaging in anatomic form. It has no traumatic characteristics and is one of the best methods to diagnose and guide the treatment of tumors at present. Ultrasound imaging is a diagnostic medical procedure that uses high-frequency sound waves to produce dynamic visual images of organs, tissues or blood flow. The experimental data are CT, MRI, PET and Ultrasound images, as shown in Fig. 4.

As shown in the Fig. 4, Fig. 4a is a CT image of the hand bone which is 99×205 pixels. Fig. 4b is a MRI of brain with Metastatic bronchitis which is 256×256 pixels, the focus is the white area in the red frame. Fig. 4c is a PET image of brain with glioma which is 256×256 pixels, the focus is the white area circling in the red frame. Fig. 4d is an Ultrasound image of intrauterine early pregnancy which is 201×201 pixels.

In addition, we also apply this method to the application of the Diffusion Tensor Imaging (DTI). The experimental DTI data are axial brain DTI slices of a normal subject, and the data is acquired from [25]. Unlike ordinary medical images, each pixel of a DTI image corresponds to a Diffusion Tensor (DT) which is a second-order rank 3 diffusion tensors with 6 unique elements, and the DT represents the water molecules diffusion at current. The DTI data is preprocessed with following specification: matrix size = 128×128, b-value = 1000 S/mm^2, and number of direction = 68 [10].

4.2. Object evaluation criteria

We verified the result from subjective visual effect and objective quality evaluation. The subjective visual effects are mainly evaluated based on the number of colors and local color contrasts. The images with more colors have more detailed image information, and the colorization effect is better. Color perception of medical image using local area block color differences highlight the different regional structure. Objective evaluation is generally described by some quantifiable evaluation indicators, in this paper, we evaluate the results according to statistical characteristics, gradient values and information volume.

Visual observation is a subjective evaluation criterion for image quality, and there is a difference in judging the quality of the same image due to differences in observers. To overcome the drawback of subjective evaluation, we use contrast, average gradient and entropy to objectively evaluate the effect of color images of CT, MRI, PET and Ultrasound. Considering the particularity of DTI data, fewer evaluation indexes can be adopted, we only use information entropy to objectively evaluate the resulting image of DTI.

The contrast ratio of the image is mainly to measure the differences between the image target and the background. The greater the contrast of the image has, the more significant the target is, so that it is more conducive to the target recognition. The contrast is defined as

$$Contrast = \sum_{\delta} \delta(i,j)^2 p_\delta(i,j). \tag{16}$$

where $\delta(i,j) = |i-j|$ denotes gray difference between adjacent pixels, $p_\delta(i,j)$ denotes the probability of pixel distribution with a gray difference of δ between adjacent pixels.

Average gradient is the clarity of the image, which reflects the improvement of image quality, the contrast of fine details and the expression of texture features in an image. The average gradient is larger, the image is clearer, the details is more abundant. The average gradient is defined as

$$\text{Average gradient} = \frac{1}{mn}\sum_{i=1}^{m}\sum_{j=1}^{n}\sqrt{\frac{\Delta xf(i,j)^2 + \Delta yf(i,j)^2}{2}}. \tag{17}$$

Where $\Delta xf(x,\ y) = f(i,\ j) - f(i+1,\ j)$ denotes the difference along x direction, the $\Delta yf(x,y) = f(i,j) - f(i,j+1)$ denotes the difference along y direction, the $mn = m \times n$ denotes image resolution. When we calculate the average gradient, we get the average gradient of the three channels of R, G, and B respectively, then we take the average of the three values as the average gradient of a color image.

Image entropy is a statistical measure of the uncertainty of the resulting image quantitatively, the lower of entropy indicates that the color information is more ordered and the complexity of the image is lower. The entropy is defined as

$$Entropy = -\sum_{i=1}^{n} P_i \log P_i. \tag{18}$$

Where the P_i denotes the probability of the probability of the gray level i in the resulting image.

4.3. Experimental results and comprehensive analysis of this results on CT, MRI, PET, Ultrasound images

After several experiments, the parameter values of the better results are selected. In the implementation of experiment on CT, MRI, PET and Ultrasound images, we set the feature weight $\omega = [0.7, 0.05, 0.05, 0.05, 0.05, 0.05, 0.05]$. We set the heat kernel $\alpha = 0.5$ and the k-NN is set to 5 while employ LE. We abbreviate literature [3,5,6,9] as TCGI [3], CTCCS [5], ACGCDT [6] and ICTED [9] respectively when doing experiments comparison.

As the results shown in Fig. 5, TCGI and ACGCDT hide parts of object which are marked by the red frame, that lead to image distortion, so they can not conducive to clinical diagnosis. Outcomes

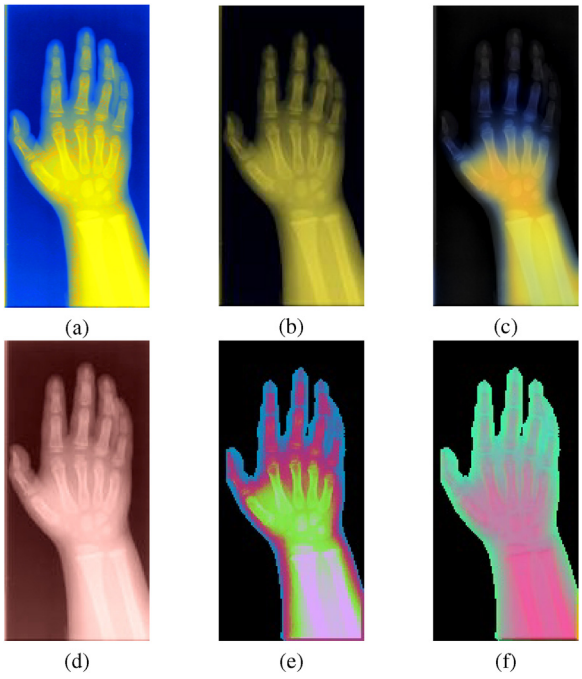

Fig. 5. Color perception of CT images. (a) TCGI [3], (b) CTCCS [5], (c) ACGCDT [6], (d) ICTED [7], (e) CPMI-DPHC(LE), (f) CPMI-DPHC(MDS). (For interpretation of the references to color in this figure legend, the reader is referred to the web version of this article.)

Table 1
Objective evaluation of CT processed by the five techniques.

Method	Contrast	Average gradient	Entropy
TCGI [3]	1172.659	1.039	7.24
CTCCS [5]	63.225	0.472	5.87
ACGCDT [6]	44.314	0.533	6.261
ICTED [9]	81.304	0.838	7.417
CPMI-DPHC(LE)	541.434	0.786	3.673
CPMI-DPHC(MDS)	546.060	0.820	3.731

of CTCCS and ICTED appear dark and the amount of color is single. Notably, our method makes the color contrast of the image intensely. This is supported by the contrast on Table 1, the contrast is far higher than the other four methods. The image processed by LE emphasizes the local structure in the image which separates the image into different blocks. The image processed by MDS protrudes detail information of the hand bone and has significant division between knuckles. Although the average gradient of our approach are lower than TCGI and ICTED, the information entropy is only half of the two methods, explaining the results of our method has lower uncertainty.

As can be seen from Fig. 6, TTCGI displays the area that is not obvious in the original medical image, but it also enhances some noises pixels. CTCCS smooths part of the focus leading to loss the crucial information of the object. ACGCDT does not use color changes to highlight the focus area and the ICTED makes poor visual. This indicates a good agreement between the observed in Fig. 4 and calculated average gradient in Table 2. Our method gives different colors to the focus and rest area, and has significant texture information, so that have higher values of average gradient and contrast. Even if the color information of our method is abundant, it still has the lowest entropy.

The values of the three objective evaluation criteria in Table 3 are roughly the same, but our approach stays ahead of the others. However, there is a big difference in vision as shown in Fig. 7. The color images gained from TCGI and ICTED are dim, they reduce the discrimination of the original medical image. CTCCS gives the original medical fine color information, which makes the detail that cannot observed by naked eyes clearly. ACGCDT has good visual effect but conceals few information in the original image. Our method has big difference between the images process by LE and MDS. The partial information of the original image is concealed, but the structure of the region is partitioned obviously in the image processed by LE. Different color is given to the original structure, but the focus cannot be easily seen in the image processed by MDS.

Fig. 8 shows pseudo color Ultrasound images obtained by TCGI, CTCCS, ACGCDT, ICTED and our method. As the Ultrasound images exist the blur of edge phenomenon, the readability of images are

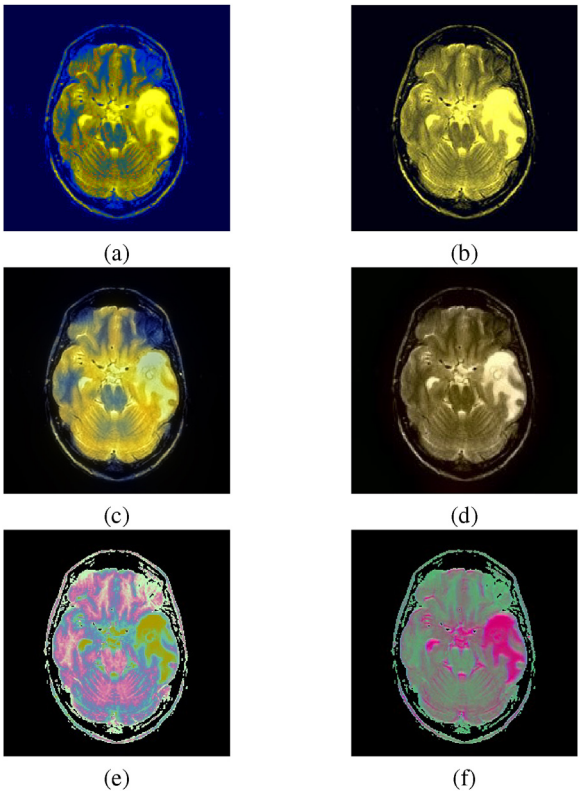

Fig. 6. Color perception of MRI images. (a) TCGI [3], (b) CTCCS [5], (c) ACGCDT [6], (d) ICTED [7], (e) CPMI-DPHC(LE), (f) CPMI-DPHC(MDS). (For interpretation of the references to color in this figure legend, the reader is referred to the web version of this article.)

Table 2
Objective evaluation of MRI processed by the five techniques.

Method	Contrast	Average gradient	Entropy
TCGI [3]	153.082	0.311	4.300
CTCCS [5]	246.371	0.271	4.448
ACGCDT [6]	116.581	0.285	5.525
ICTED [9]	68.885	0.221	5.120
CPMI-DPHC(LE)	1277.800	0.422	3.059
CPMI-DPHC(MDS)	631.360	0.319	2.987

Table 3
Objective evaluation of PET processed by the five techniques.

Method	Contrast	Average Gradient	Entropy
TCGI [3]	71.605	0.183	5.188
CTCCS [5]	134.616	0.310	5.427
ACGCDT [6]	52.831	0.2713	5.518
ICTED [9]	43.339	0.242	5.76
CPMI-DPHC(LE)	231.692	0.373	4.139
CPMI-DPHC(MDS)	138.577	0.349	4.373

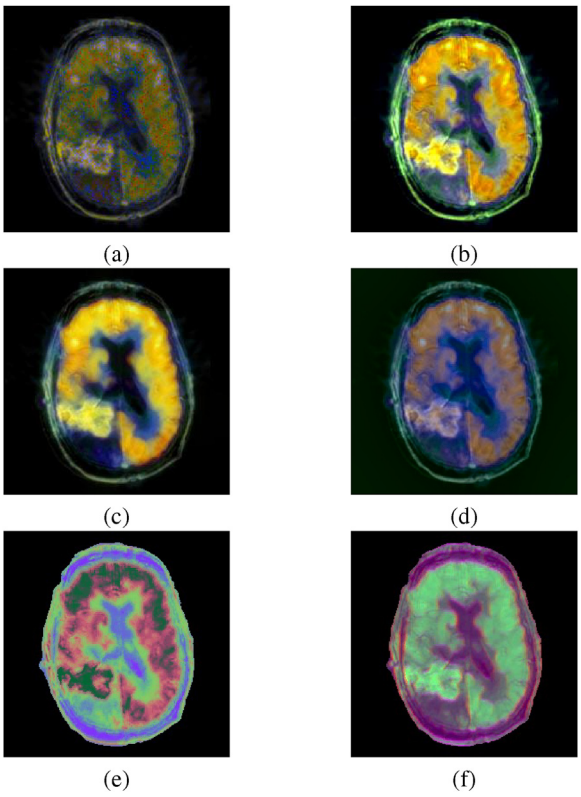

Fig. 7. Color perception of PET images. (a) TCGI [3], (b) CTCCS [5], (c) ACGCDT [6], (d) ICTED [7], (e) CPMI-DPHC(LE), (f) CPMI-DPHC(MDS). (For interpretation of the references to color in this figure legend, the reader is referred to the web version of this article.)

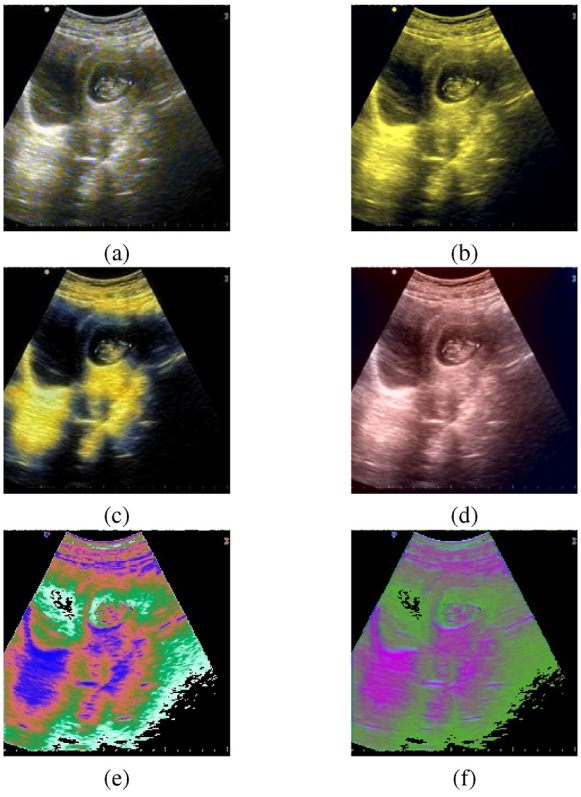

Fig. 8. Color perception of ultrasound images. (a) TCGI [3], (b) CTCCS [5], (c) ACGCDT [6], (d) ICTED [7], (e) CPMI-DPHC(LE), (f) CPMI-DPHC(MDS). (For interpretation of the references to color in this figure legend, the reader is referred to the web version of this article.)

Table 4
Objective evaluation of Ultrasound processed by the five techniques.

Method	Contrast	Average gradient	Entropy
TCGI [3]	232.270	0.431	6.773
CTCCS [5]	210.526	0.351	6.243
ACGCDT [6]	156.694	0.354	5.861
ICTED [9]	186.085	0.443	7.162
CPMI-DPHC(LE)	1629.910	0.651	4.946
CPMI-DPHC(MDS)	437.078	0.503	4.422

less improved after processed by those methods. In the TCGI and ICTED, the images have faint color, so that the visual effect are worse. CTCCS gives image color information, but details are vague, this is consistent with the observation from the lowest average gradient in the Table 4. The ACGCDT has poor contrast is supported by the image obtained by ACGCDT, it appears a lot of black color as the background. The image processed by LE has particularly huge values of contrast and average gradient; coincided with its obvious edge and variety colors. Although our method increases the overall outline of image, it weakens the fetal information of this image slightly as well. In spite of the rich color of our method, the image information is more orderly in vision. The results are in good consistent with the lower entropy.

4.4. Experimental results and comprehensive analysis of this results on DTI

Multi-feature extraction is not needed in virtue of the processed DTI data already have plentiful high dimensional information, so the dimension of pixel features vector is six which represents six independent elements corresponding to every pixel. And also there is no need to set the feature weight. In this section, we compare the proposed method with fractional anisotropy (FA), DPDR and CPDTI-HML. Since CPDTI-HML has a level of selection, taking into account the comparability of the experiment, we choose the experimental results of its sixth and seventh layers to compare with the proposed method. Set the kernel parameter as 0.5 and the k of k-nearest neighbor as 5 when using LE to process data.

As is show in the Fig. 9. The DPDR has contrasting color combinations and harsh edges, so that cannot express the different areas by color accurately. The CPDTI-HML expresses the regional structure clearly, but there is few noise in the object of the image. Our method not only expresses the edges clearly, but also shows more details in the image.

Comparison of FA, DPDR, CPDTI-HML and our method in Fig. 10. The outcome of DPDR has protruded outline of the structure but the middle part texture is unclear. The CPDTI-HML has rich color but it is chaotic. Different from them, our method not only reflects the underlying structure with different colors, but also possesses fine details.

Fig. 11 shows the results of FA, DPDR, CPDTI-HML and our method applies to DTI slice 1. The regional information gets lost in the clutter because of the multicolor which produced by DPDR. The CPDTI-HML can reflect the underlying structure effectively. Our method has better detailed structural and textural information than DPDR and CPDTI-HML.

Comparison of FA, DPDR, CPDTI-HML and our method in Fig. 12. The DPDR cannot distinct different structures visibly. The outcome of CPDTI-HML has noise immunity, and highlight different areas with dissimilar color. Our method not only has obvious boundaries but also allows colors to run bolder and fuller.

Table 5 provides details of entropy of FA, DPDR, CPDTI-HML and our method. As can be seen from the Table 5, the entropy of the images that obtained from our method are obviously lower than FA and DPDR. By comparison, very little difference between CPDTI-HML with our approach. This parameter is verifying the conclusion

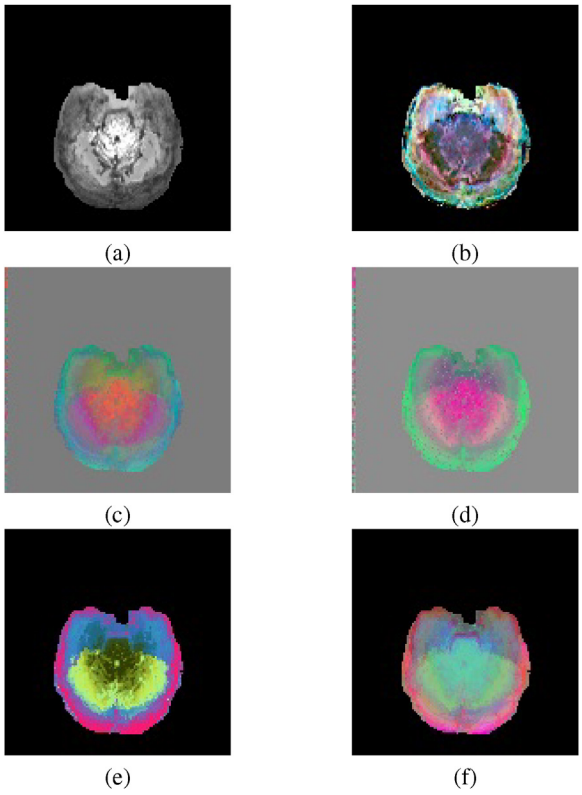

Fig. 9. Color perception of DTI slice 1. (a) FA, (b) DPDR [7], (c) CPDTI-HML(sixth layer) [10], (d) CPDTI-HML(seventh layer) [10], (e) CPMI-DPHC(LE), (f) CPMI-DPHC(MDS). (For interpretation of the references to color in this figure legend, the reader is referred to the web version of this article.)

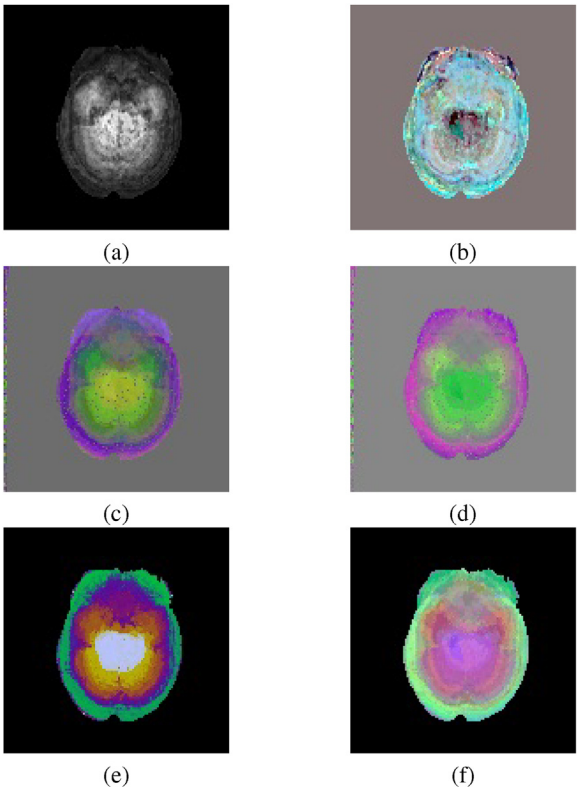

Fig. 11. Color perception of DTI slice 3. (a) FA, (b) DPDR [7], (c) CPDTI-HML(sixth layer) [10], (d) CPDTI-HML(seventh layer) [10], (e) CPMI-DPHC(LE), (f) CPMI-DPHC(MDS). (For interpretation of the references to color in this figure legend, the reader is referred to the web version of this article.)

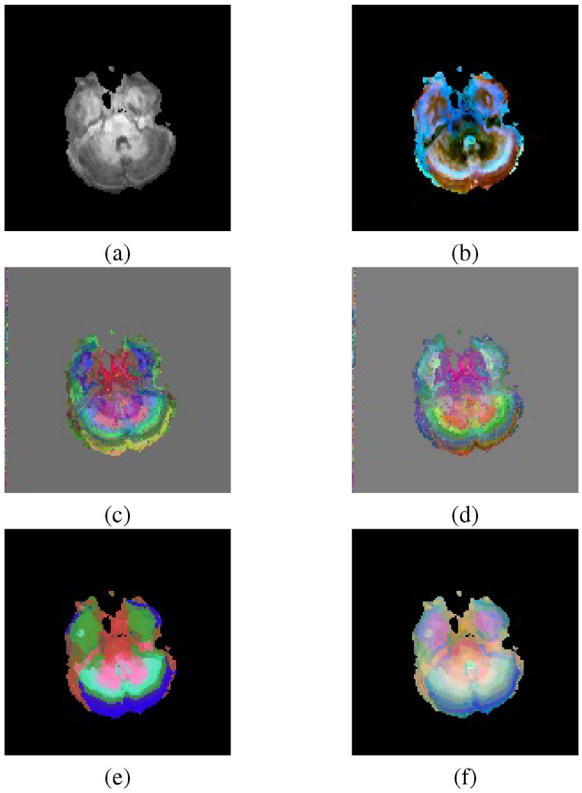

Fig. 10. Color perception of DTI slice 2. (a) FA, (b) DPDR [7], (c) CPDTI-HML(sixth layer) [10], (d) CPDTI-HML(seventh layer) [10], (e) CPMI-DPHC(LE), (f) CPMI-DPHC(MDS). (For interpretation of the references to color in this figure legend, the reader is referred to the web version of this article.)

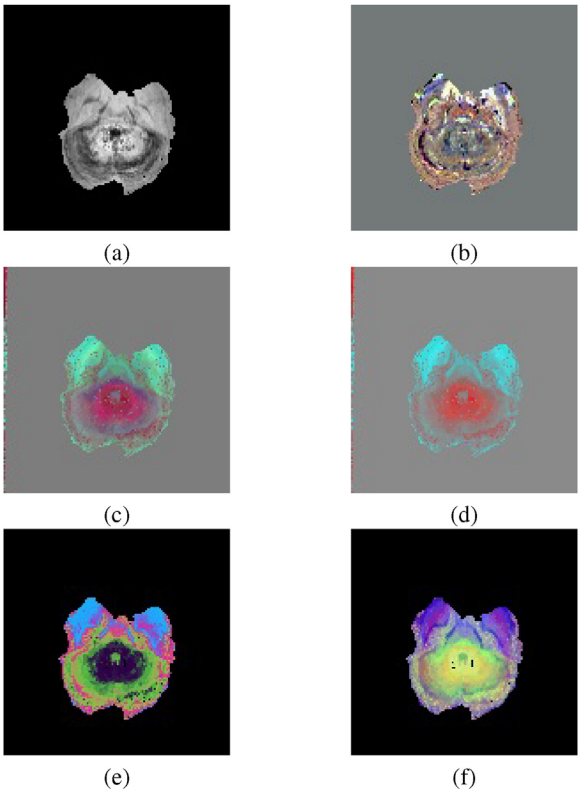

Fig. 12. Color perception of DTI slice 4. (a) FA, (b) DPDR [7], (c) CPDTI-HML(sixth layer) [10], (d) CPDTI-HML(seventh layer) [10], (e) CPMI-DPHC(LE), (f) CPMI-DPHC(MDS). (For interpretation of the references to color in this figure legend, the reader is referred to the web version of this article.)

Table 5
The entropy of the four techniques.

Method	Slice1	Slice2	Slice3	Slice4
FA	2.723	2.118	3.078	2.148
DPDR [7]	2.786	2.181	2.959	2.146
CPDTI-HML(sixth layer) [10]	2.055	2.030	2.742	2.073
CPDTI-HML(seventh layer) [10]	2.331	2.040	2.648	1.922
CPMI-DPHC(LE)	2.402	1.953	2.763	1.926
CPMI-DPHC(MDS)	2.366	1.999	2.734	2.086

Table 6
The average expert score of the results of common medical images.

Method	CT	MRI	PET	Ultrasound
TCGI [3]	2.00	3.00	3.33	3.67
CTCCS [5]	2.67	3.33	2.67	1.33
ACGCDT [6]	3.33	3.33	3.00	2.33
ICTED [9]	2.33	3.67	3.67	1.33
CPMI-DPHC(LE)	1.67	1.33	1.33	3.67
CPMI-DPHC(MDS)	1.67	1.67	1.67	3.67

Table 7
The average expert score of the four techniques.

Method	Slice1	Slice2	Slice3	Slice4
FA	3.67	3.67	3.67	3.67
DPDR [7]	3.33	3.00	3.33	3.67
CPDTI-HML(sixth layer) [10]	3.00	3.00	2.67	3.00
CPDTI-HML(seventh layer) [10]	2.67	2.00	2.33	2.67
CPMI-DPHC(LE)	1.33	1.00	1.67	1.33
CPMI-DPHC(MDS)	1.33	1.33	1.00	1.33

that our method ensures the low uncertainty and fine details while improving the visual effect.

4.5. Qualitative evaluation criterion

Besides, the qualitative evaluation criterion is imported. We display the result to three experts (radiologists), then ask them to evaluate the results (Very good = 1, Good = 3, Fair = 3, and Bad = 4) and average the results shown in Table 6. All the experts are from class-A major hospital in Chongqing, China. Two of them are the director doctor of the Department of Radiology and another comes from the Department of Ultrasound.

Table 6 shows the score of our method are highest except for Ultrasound images, which means that experts are approve the results of CT, MRI and PET, but not satisfied with that of the Ultrasound. The results in Table are consistent with objective evaluation criteria, i.e., experts prefer the results which have preferably objective evaluation value. Also, it proves the validity of objective evaluation indicators indirectly.

Table 7 provides details of average expert score of FA, DPDR, CPDTIHML and our method. It is clear that the proposed method gains the average expert score between 1 and 1.67, which means there are more than two experts scored 'very good' or 'good'. Table 7 also explains the proposed method possessed sufficient feasibility and relatively high utility value, which would effectively assists for medical diagnosis.

5. Discussion

Here, we elucidate some discussions about the proposed method for color perception of medical images based on multi-feature fusion and hierarchical density peaks clustering, which reduces the complex computation from $O(N^3)$ (DPDR) to $O(MN)$. The experimental results verify the feasibility and rationality of the proposed method from different aspects. On the one hand, most of ordinary medical images and DTI processed by the proposed method have diversified colors and rich details. We utilize the hierarchical density peak clustering algorithm to gain the representative pixels, which can not only retain the regional structure information of the image, but also reduce the computational complexity of subsequent processing. When clustering the pixels, the various gradient features we seek provide rich image area information and edge information to ensure more accurate classification. In addition, we use rotation scale to maximize the color gamut and volume among the representative pixels. And then the perceptual color differences are highlighted and the color information between the representative pixels is enriched. On the other hand, as for the qualitative evaluation, experts have stronger recognition for our method compared with other methods. It means that the proposed method can generate more easy-understanding medical images, which is helpful for medical diagnosis and studies.

Reducing the dimension with MDS can make the color of the pixels with short distance more similar and the color of the pixels with long distance more distinguishing. Reducing the dimension with LE can make the color of adjacent pixels more similar, so that the regional information is obvious. From the experiments we can arrive at the conclusion that the neighborhood preserving embedding may not be a suitable option for our method. The results of the experiment prove this hypothesis.

However, there are still some defects of the method. For example, in the Ultrasound images, our method uses the contrast colors to create a better visual effect, but the focal area is not obvious. The inherent spackle noise of ultrasound images makes the feature extraction difficult, and the gradient operator is so sensitive to noise that the results of the Ultrasound image are inferior. In the future work, we can de-noise the medical image before the feature extraction to reduce the interference of noise and to guarantee the quality of image edge. Also, we can use the image transformation techniques to unite into discontinuous edge information into finer edge information. Besides, other feature extraction methods can be used to improve our method, such as feature extraction based on Deep Neural Network.

6. Conclusions

In this work, we present a new method for color perception of medical images based on multi-feature fusion and hierarchical density peak clustering. This method is advantageous in some aspects like visual information and algorithm efficiency compared with DPDR. We use Nevatia operator to extract multi-direction gradient features which used to construct high dimensional data from medical images, so that we can generate color medical images that has exquisite details and clear texture information. Furthermore, we utilize the density peak based hierarchical clustering to select the regional representative pixels, it reduces the complex computation from $O(N^3)$ to $O(MN)$. In addition, the proposed method can not only be used to process DTI but also extends to ordinary grayscale medical images. For clinical application, the proposed method can offer better visualization of grayscale medical image with clear regional structures and fine textures, and it can help doctors to analyze and diagnose diseases. On the other hand, so far, this approach does not achieve better visual for all modalities of medical images. Therefore, the proposed method can be optimized in feature extraction and the selection of representative pixels in future research.

Acknowledgement

The author would like to thank the anonymous reviewers for their help. The author also would like to thank the director doctor Shuxia Sun and the deputy director doctor Changqing Duan in the Radiology Department of Jiulongpo District Hospital of Tradi-

tional Chinese Medicine, Chongqing, China, and the doctor Jie Yang in the Ultrasound Department of Chongqing Rongchang District Hospital of Traditional Chinese Medicine, Chongqing, China. This work was supported by the National Natural Science Foundation of China (Grant No. 61672120), the Chongqing Natural Science Foundation Program (Grant No. cstc2015jcyjA40036) and Postgraduate Scientific Research and Innovation Project of Chongqing (Grant No. CYS17224).

References

[1] P. Bhargavi, C.H. Bindu, K. Veeraswamy, K.S. Prasad, A novel medical image fusion with l color transformation, in: ICCCI, IEEE, 2015, pp. 1–6.
[2] A. Sharma, M. Kaur, Enhanced false coloring in medical image processing, Int. J. Adv. Res. Ideas Innov. Technol. 3 (1) (2017) V3I1–1168.
[3] T. Welsh, M. Ashikhmin, K. Mueller, Transferring color to greyscale images, ACM Trans. Graphics 21 (3) (2002) 277–280.
[4] A. Brun, H.J. Park, H. Knutsson, C.F. Westin, Coloring of DT-MRI fiber traces using laplacian eigenmaps, in: EUROCAST, Springer, 2003, pp. 518–529.
[5] X. Xiao, L. Ma, Color transfer in correlated color space, in: VRCAI, ACM, 2006, pp. 305–309.
[6] F. Pitié, A.C. Kokaram, R. Dahyot, Automated colour grading using colour distribution transfer, Comput. Vis. Image Understand. 107 (1–2) (2007) 123–137.
[7] G. Hamarneh, C. Mcintosh, M.S. Drew, Perception-based visualization of manifold-valued medical images using distance-preserving dimensionality reduction, IEEE Trans. Med. Imaging 30 (7) (2011) 1314–1327.
[8] Z.G. Zhu, Y.Y. Kong, Visualization of diffusion tensor images using locality preserving dimensionality reduction, Chin. Med. Equip. J. 34 (6) (2013) 20–22.
[9] L. He, H. Qi, R. Zaretzki, Image color transfer to evoke different emotions based on color combinations, Signal Image Video Process. 9 (8) (2015) 1965–1973.
[10] X. Zeng, S. He, W. Li, Color prception of diffusion tensor images using hierarchical manifold learning, Pattern Recognit. 63 (2017) 583–592.
[11] C.W. Kok, Y. Hui, T.Q. Nguyen, Medical image pseudo coloring by wavelet fusion, in: EMBS, IEEE, 1996, pp. 648–649.
[12] A. Rodriguez, A. Laio, Clustering by fast search and find of density peaks, Science 344 (6191) (2014) 1492.
[13] A. Abbasloo, V. Wiens, M. Hermann, T. Schultz, Visualizing tensor normal distributions at multiple levels of detail, IEEE Trans. Vis. Comput. Graphics 22 (1) (2015) 975–984.
[14] J.B. Kruskal, Multidimensional scaling by optimizing goodness of fit to a nonmetric hypothesis, Psychometrika 29 (1) (1964) 1–27.
[15] L. Yang, B.L. Guo, W. Ni, Multimodality medical image fusion based on multiscale geometric analysis of contourlet transform, Neurocomputing 72 (1) (2008) 203–211.
[16] X.B. Liu, W.B. Mei, H.Q. Du, Multi-modality medical image fusion based on image decomposition framework and nonsubsampled shearlet transform, Biomed. Signal Process. Control 40 (2018) 343–350.
[17] D.E. Nirmala, V. Vaidehi, Comparison of pixel-level and feature level image fusion methods, in: ICSD, IEEE, 2015, pp. 743–748.
[18] R. Nevatia, K. Ramesh Babu, Linear feature extraction and description, Comput. Graphics Image Process. 13 (1980) 257–269.
[19] J. Xu, G. Wang, W. Deng, DenPEHC: density peak based efficient hierarchical clustering, Inf. Sci. 373 (12) (2016) 200–218.
[20] Z.H. Zhou, Machine Learning, Tsinghua University Press, 2016, pp. 237–241.
[21] S. Umeyama, Least-squares estimation of transformation parameters between two point patterns, IEEE Trans. Pattern Anal. Mach. Intell. 13 (4) (1991) 376–380.
[22] L. Anany, Introduction to the Design and Analysis of Algorithms, Tsinghua University Press, 2007, pp. 359–365.
[23] M. Belkin, P. Niyogi, Laplacian eigenmaps for dimensionality reduction and data representation, Neural Comput. 15 (6) (2003) 1373–1396.
[24] http://www.med.harvard.edu/AANLIB/home.htm.
[25] https://www.nlm.nih.gov/research/visible/photos.html.